

# Biomechanical remodeling of the murine descending thoracic aorta during late-gestation pregnancy

Ana I. Vargas<sup>a</sup>, Samar A. Tarraf<sup>a</sup>, Timothy P. Fitzgibbons<sup>b</sup>, Chiara Bellini<sup>a,1,\*\*</sup>,  
Rouzbeh Amini<sup>a,c,1,\*</sup>

<sup>a</sup> Department of Bioengineering, Northeastern University, Boston, MA, 02115, United States

<sup>b</sup> Department of Medicine, Division of Cardiovascular Medicine, University of Massachusetts Medical School, Worcester, MA, 01655, United States

<sup>c</sup> Department of Mechanical and Industrial Engineering, Northeastern University, Boston, MA, 02115, United States

## ARTICLE INFO

### Keywords:

Aortic distensibility  
Aortic stiffness  
Late gestation  
Law of Laplace  
Normotensive pregnancy  
Tensile wall stress

## ABSTRACT

With the rise in maternal mortality rates and the growing body of epidemiological evidence linking pregnancy history to maternal cardiovascular health, it is essential to comprehend the vascular remodeling that occurs during gestation. The maternal body undergoes significant hemodynamic alterations which are believed to induce structural remodeling of the cardiovascular system. Yet, the effects of pregnancy on vascular structure and function have not been fully elucidated. Such a knowledge gap has limited our understanding of the etiology of pregnancy-induced cardiovascular disease. Towards bridging this gap, we measured the biaxial mechanical response of the murine descending thoracic aorta during a normotensive late-gestation pregnancy. Non-invasive hemodynamic measurements confirmed a 50% increase in cardiac output in the pregnant group, with no changes in peripheral blood pressure. Pregnancy was associated with significant wall thickening (~14%), an increase in luminal diameter (~6%), and material softening in both circumferential and axial directions. This expansive remodeling of the tissue resulted in a reduction in tensile wall stress and intrinsic tissue stiffness. Collectively, our data indicate that an increase in the geometry of the vessel may occur to accommodate for the increase in cardiac output and blood flow that occurs in pregnancy. Similarly, wall thickening accompanied by increased luminal diameter, without a change in blood pressure may be a necessary mechanism to decrease the tensile wall stress, and avoid pathophysiological events following late gestation.

## 1. Introduction

During the nine months of gestation, the maternal body undergoes significant hemodynamic alterations, potentially inducing structural remodeling of the cardiovascular system (Wells and Martin, 2022; Pierlot et al., 2014, 2015). Combined with the drastic hemodynamic changes, the growing fetus applies additional forces which place a burden on the maternal cardiovascular system, revealing previously undiagnosed cardiovascular problems (Ramalakhan et al., 2020). Cardiovascular disease (CVD) complicates about 4% of pregnancies globally (Duley, 2009; Regitz-Zagrosek et al., 2018). In the U.S., CVD accounts for more than one-third of pregnancy-related deaths, making cardiovascular complications the leading cause of maternal mortality (Petersen et al., 2019).

During a normotensive pregnancy, i.e., a pregnancy with normal blood pressure levels, the maternal body is presented with cardiovascular challenges due to the significant hemodynamic changes that occur during gestation. Fig. 1 provides a summary of the maternal hemodynamic changes associated with gestation time from multiple studies (Robson et al., 1989; Grindheim et al., 2012; Katz et al., 1978; Clapp and Capeless, 1997; Kager et al., 2009; Poppas et al., 1997; Zentner et al., 2012; Rodriguez et al., 2018; Huisman et al., 1987; Oosterhof et al., 1993; Buchan, 1984; Mulder et al., 2022). During the course of pregnancy, the mother's blood pressure and pulse pressure (Fig. 1A and B) do not change significantly, while the cardiac output is observed to increase by approximately 45% at late gestation (Fig. 1C) (Hunter and Robson, 1992). Similarly, maternal blood volume increases by approximately 40% by the end of gestation (data not shown) (Thornburg et al., 2000).

\* Corresponding author. Department of Bioengineering, Northeastern University, 360 Huntington Ave. Boston, MA, 02125, USA.

\*\* Corresponding author.

E-mail addresses: [c.bellini@northeastern.edu](mailto:c.bellini@northeastern.edu) (C. Bellini), [r.amini@northeastern.edu](mailto:r.amini@northeastern.edu) (R. Amini).

<sup>1</sup> These authors contributed equally to this work.

In addition, blood viscosity (Fig. 1D) decreases during mid gestation and rises to normal levels at late gestation, which is associated with an observed 34% drop in peripheral resistance (Fig. 1E). Due to the drastic increase in cardiac output and blood volume, in spite of constant blood pressure, it is evident that the maternal arteries have to remodel to accommodate the changes in flow and volume (Wells and Martin, 2022).

Aortic compliance has previously been reported in humans as a representative measure of aortic remodeling during pregnancy (Fig. 1F). However, to the best of our knowledge, changes in aortic compliance throughout pregnancy have not been fully elucidated, with the few studies available showing inconsistent results (Poppas et al., 1997; Kager et al., 2009; Rodriguez et al., 2018). The structural stiffness of the aorta, a measure of vessel wall elasticity, has been assessed clinically using pulse wave velocity (PWV) throughout human gestation. Franz et al. (2013) measured the PWV of normotensive pregnancies and concluded that PWV increased during late gestation, indicating aortic stiffening. Similarly, Osman et al. (2017), reported that PWV initially

declined during the first trimester and increased in the third trimester. However, conflicting results have been reported in other studies. In particular, aortic PWV decreased from early gestation to late gestation, indicating a decline in the structural stiffness (Mersich et al., 2005; Turi et al., 2020). Inconsistent reports of maternal aortic stiffness highlight a critical gap in our understanding of the structural remodeling of the aortic wall during pregnancy. In particular, aortic stiffening has been implicated in the pathogenesis of complicated hypertensive pregnancies due to preeclampsia (Torrado et al., 2015; Estensen et al., 2013) and connective tissue disorders such as Marfan's Syndrome (Groenink et al., 1998; Jondeau et al., 1999). Stiffness plays a crucial role in arterial function by influencing the energy stored in the arterial wall under physiological deformation of the vessel. Normally, the elasticity of the arterial wall allows it to act as an elastic reservoir, distending—and storing elastic energy—during cardiac systole and then recoiling—and releasing the stored energy—during diastole, thereby augmenting blood flow through the Windkessel effect. However, when the arterial wall

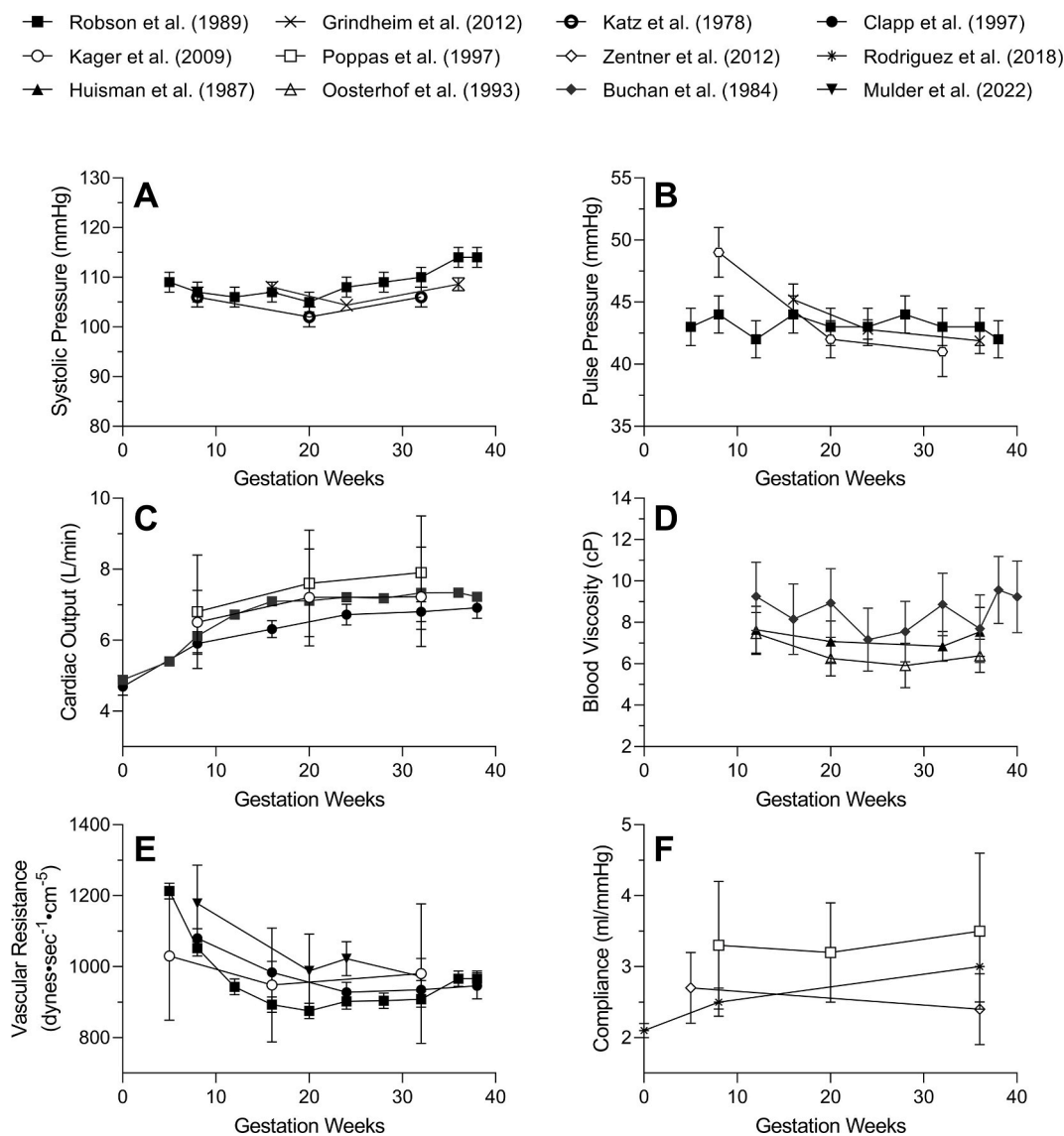


**Fig. 1.** Literature review on maternal hemodynamics during pregnancy (Robson et al., 1989; Grindheim et al., 2012; Katz et al., 1978; Clapp and Capeless, 1997; Kager et al., 2009; Poppas et al., 1997; Zentner et al., 2012; Rodriguez et al., 2018; Huisman et al., 1987; Oosterhof et al., 1993; Buchan, 1984; Mulder et al., 2022). (A) Systolic blood pressure and (B) pulse pressure remain constant throughout pregnancy. (C) Cardiac output increases ( $r_s = 0.766, P < 0.001^*$ ). (D) Blood viscosity decreases and rises to normal levels during late gestation. (E) Vascular resistance decreases during gestation ( $r_s = -0.579, P = 0.005^*$ ). (F) The trend on the behavior of arterial compliance during gestation is not consistent (or clear) among different studies. We relied on the Pearson correlation coefficient test to determine the level of correlation between the two variables in a linear manner. The  $r_s$  values indicate the strength and direction of the correlation, with  $P < 0.05$  considered a statistically significant correlation.

becomes stiffer, it loses its ability to distend elastically, compromising its capacity to store and release energy. As a result, the continuous perfusion of blood flow is disrupted, leading to other cardiovascular complications (Wagenseil and Mecham, 2009; Cociolone et al., 2018). Therefore, accurately quantifying aortic wall stiffness is an essential step in bridging our knowledge gap with regards to vascular remodeling in normal and hypertensive pregnancies.

Because PWV takes into account both shape and material properties of the aorta, it is impossible to identify whether changes in the structural stiffness are due to either alterations in the intrinsic mechanical properties of the wall, changes in geometry, changes in loading, or a combination thereof. Differentiating between these factors, and their specific contribution to the structural stiffness of the vessel wall, is important to fully elucidate the remodeling that occurs during pregnancy.

To identify the functional changes that occur in the aorta during pregnancy, we quantified the biaxial mechanical properties of the murine descending thoracic aorta (DTA) during a normotensive late-gestation pregnancy. The detailed characterization of these mechanical properties is necessary to assess changes in intrinsic behavior and link the quantified tissue responses to clinical observations of normotensive pregnancies. Given the preserved blood pressure coupled with the increased cardiac output throughout gestation, one could postulate that the central vasculature undergoes a remodeling process to maintain a homeostatic stress state despite an increase in blood flow. As such, we hypothesized that the DTA wall stress remains unchanged during late-gestation normotensive pregnancies. Moreover, our study provides a baseline characterization of normotensive pregnancies that may be used in future studies to assess risk of CVD and to examine vascular remodeling mechanisms associated with complicated pregnancies.

## 2. Methods

### 2.1. Animals and sample groups

Experimental procedures involving animals followed National Institutes of Health (NIH) guidelines and received Northeastern University Institutional Animal Care and Use Committee (IACUC) approval. Pregnant C57BL/6 mice ( $n = 9$ ) at gestation day  $18 \pm 1$  were assigned to the late-gestation group. Gestation day 18 was selected as it is roughly equivalent to being 197 days pregnant in humans, which falls within the third trimester of pregnancy (Blum et al., 2017; Davidson, 1989). C57BL/6 nulligravida female mice ( $n = 9$ ) served as the non-pregnant, age-matched controls ( $10 \pm 1$  weeks of age).

### 2.2. Hemodynamic measurements

Blood pressure measurements were collected in awake, restrained mice ( $n = 9$  for both groups) using a non-invasive tail-cuff system (CODA; Kent Scientific, Torrington, CT). One blood pressure measurement for the pregnant group was excluded due to inaccurate/extreme measurements.

Additional 10-week-old pregnant (day 15-17 of gestation) and non-pregnant, age-matched C57BL/6 female mice ( $n = 3$  per group) were purchased from Jackson Laboratories (Bar Harbor, ME) and delivered to the UMass Chan Medical School Cardiovascular & Surgical Models Core (IACUC #20220006) for ultrasound imaging. The abdomen and chest were treated with depilatory cream. Animals were induced with 2.0% isoflurane mixed with 0.5L/min 100%  $O_2$  and gently affixed to the heated physiologic platform of the Vevo 3100 imaging system (Visualsonics, Toronto, ON, Canada). Electrode cream was applied to each limb. Body temperature was continually monitored and maintained at  $37^\circ\text{C}$  with a rectal temperature probe. Isoflurane was administered by nose cone and the concentration was reduced to 1.0% isoflurane mixed with 0.5L/min 100%  $O_2$  for maintenance. All animals were imaged at a heart rate (HR) of at least 450-500 beats per minute. Two dimensional (2D)

and M-mode images were obtained in the parasternal long and parasternal short axis with a 50 MHz transducer (MX550S), as previously described (Respress and Wehrens, 2010; Scherrer-Crosbie and Thibault, 2008). Image analysis was performed off-line using the VevoLab image analysis software. Left ventricular volumes at end-diastole ( $LV_d$ ) and end-systole ( $LV_s$ ) were derived from M-mode measurements using Teichholz's formula,

$$LV_d = \frac{7.0(LVID_d)^3}{2.4 + LVID_d} \quad (1)$$

$$LV_s = \frac{7.0(LVID_s)^3}{2.4 + LVID_s} \quad (2)$$

where  $LVID_d$  and  $LVID_s$  represent the left ventricular internal dimensions at end-diastole and end-systole, respectively. Stroke volume (SV) measurements were used to calculate the cardiac output (CO) of each mice, such that

$$SV = LV_d - LV_s \quad (3)$$

$$CO = \frac{SV * HR}{1000} \quad (4)$$

### 2.3. Sample collection and preparation

After completion of blood pressure measurements, mice were euthanized and a ~5-mm segment of the DTA was excised. The sample was cleaned from perivascular tissue and excess fat. The lateral branches of the tissue were tied with 9-0 nylon suture. Specimens were cannulated on the proximal and distal ends onto custom-made glass micro-pipettes using 6-0 silk suture in double knots. Ring samples were taken from the proximal end of each specimen, and imaged with a dissection microscope at  $\times 45$  magnification to estimate the unloaded wall thickness using a custom MATLAB (MathWork, Natick, MA) code.

### 2.4. Passive biaxial mechanical testing

Details of the methods for the biaxial mechanical testing procedure have been reported previously (Farra et al., 2021). Briefly, prepared samples were cannulated at both ends and mounted onto a custom-made biaxial testing system for inflation/extension loading (Gleason et al., 2004) controlled by a computer. Tissues were submerged in a Hank's Balanced Solution (HBSS) bath. To measure the outer diameter of the specimens, a camera was positioned in front of the transparent HBSS bath. The distance between the two cannulae, and in turn the axial stretch of the tissue, were controlled by linear actuators mounted on the stage of the device. To measure the force resisting axial stretching, a load cell with a wire hook was attached to the distal cannula using paraffin wax. A custom LabView computer interface (National Instruments, Austin, TX) was employed to set the luminal pressure and axial length, as well as to visualize the acquired diameter and force data.

Once the tissue was mounted, the in-vivo axial stretch was estimated by identifying the specific axial stretch where the axial force remained constant within the physiological pressure range between 80 and 120 mmHg (Weizsäcker et al., 1983). At this stretch, the tissue samples then underwent a 15-minute acclimation period, during which the vessel was subjected to a pulsatile pressurization between 80 and 120 mmHg. Additionally, tissue samples underwent four cycles of preconditioning, where the luminal pressure was gradually decreased to 10 mmHg and then increased up to 140 mmHg.

Following acclimation and preconditioning, the in-vivo axial stretch was re-estimated and samples were subjected to pressure-diameter and force-length loading tests (Gleason et al., 2004). During the pressure-diameter test, samples were stretched to their estimated in-vivo axial stretch and subjected to a range of luminal pressures from 10 to 140 mmHg. The test was also repeated at a slightly lower stretch (5%

below in-vivo stretch) and a slightly higher stretch (5% above in-vivo stretch). Throughout the test, the stretch remained constant while, the pressure was gradually increased/decreased. In the force-length tests, the luminal pressure within the artery was maintained at either 10, 60, 100, or 140 mmHg. At the same time, arterial samples were stretched to obtain specific axial force values within a target range (from -0.5 g up to 5 g). Both pressure-diameter and force-length tests comprised of two cycles, the first cycle being a preconditioning cycle, and data collected on the second cycle.

## 2.5. Mechanical analysis

To measure the mechanical behavior of the arterial wall, we analyzed the stress-stretch responses of the tissue.

First, circumferential stretch ( $\lambda_\theta$ ) and axial stretch ( $\lambda_z$ ) were calculated:

$$\lambda_\theta = \frac{r + h/2}{R + H/2} \quad \text{and} \quad \lambda_z = \frac{l}{L} \quad (5)$$

where the variables  $r$ ,  $h$ , and  $l$  represent the luminal radius, thickness, and length, respectively, in the deformed/loaded configuration. Similarly, the variables  $R$ ,  $H$ , and  $L$  correspond to the same metrics in the unloaded configuration. The luminal radius and thickness of the vessel were computed using experimental values of the loaded outer diameter, and the axial length was calculated by assuming incompressibility of the tissue (i.e., constant volume).

The circumferential stress was then calculated using the law of Laplace:

$$\sigma_{\theta\theta} = \frac{Pr}{h} \quad (6)$$

The law of Laplace describes the relationship between the normal stress (i.e., normal force per unit area) exerted on the aortic wall, the pressure ( $P$ ) within the lumen, and the curvature of the wall (see [Appendix A](#) for more details). Additionally, the axial stress was computed as

$$\sigma_{zz} = \frac{f}{\pi h(2r + h)} \quad (7)$$

where  $f$  is the total axial load on the aortic wall, considering the contribution of transmural pressure.

Following well-established methods ([Ferruzzi et al., 2013](#)), the stress-stretch data were then fitted via non-linear regression to a microstructurally motivated strain-energy function to relate the stored energy in the vessel to its deformation and obtain material parameters.

Using such fitted parameters, structural and material metrics, e.g., the linearized stiffness, were estimated at experimentally obtained values of systolic blood pressure and in-vivo axial stretch, as described in detail previously ([Baek et al., 2007](#); [Farra et al., 2021](#)).

Lastly, distensibility ( $D$ ), a measure of structural stiffness often used in clinical studies, was calculated using systolic and diastolic blood pressure (i.e.,  $P_{sys}$  and  $P_{dias}$ , respectively), and systolic and diastolic inner diameters, (i.e.,  $d_{i,sys}$  and  $d_{i,dias}$ , respectively):

$$D = \frac{d_{i,sys} - d_{i,dias}}{d_{i,sys}(P_{sys} - P_{dias})} \quad (8)$$

## 2.6. Statistics

Unless specified, data are reported as mean  $\pm$  standard error of mean (SEM). Normal distribution for all data was assessed using D'Agostino and Pearson test for all samples, except for cardiac output measurements, which were too limited to be assessed for normality. As such, statistical significance was determined by Mann-Whitney-Wilcoxon unpaired sample test ([Cardillo, 2009](#)) for cardiac output measurements, and pregnant versus control data relied on Student's t-test with

two-tailed distributions. Differences in data were considered to be statistically significant if  $P \leq 0.05$ .

## 3. Results

### 3.1. Murine hemodynamics

In-vivo echocardiatic measurements confirmed an increase in cardiac output ([Fig. 2A](#)) in late-gestation pregnant mice, with average values of  $12.9 \pm 0.6$  and  $19.4 \pm 3.6$  mL/min in control and pregnant mice, respectively ( $P = 0.05$ ). Peripheral blood pressure measurements did not show any difference between groups, with average systolic ([Fig. 2B](#)), diastolic, and mean values of  $118 \pm 3$ ,  $89 \pm 6$ , and  $98 \pm 6$  mmHg for the control group, and  $113 \pm 8$ ,  $82 \pm 9$ , and  $96 \pm 8$  mmHg, for the pregnant group, respectively ( $P > 0.05$ ).

### 3.2. Aorta mechanics

Pregnancy was associated with a rightward shift of the stress-stretch curve in both circumferential and axial directions ([Fig. 3A](#) and [B](#)), suggesting tissue softening. This shift indicates that the pregnant DTA experiences a larger stretch than the control DTA at the same amount of applied stress.

Overall material softening, without a significant change in blood pressure, imposed a larger circumferential stretch at systole in the pregnant aorta ([Fig. 4A](#)) ( $1.62 \pm 0.05$  and  $1.70 \pm 0.06$ , for control and pregnant samples, respectively,  $P < 0.05$ ). Concurrently, at group-specific systolic blood pressure, the pregnant aorta was observed to have a greater luminal diameter ([Fig. 4G](#)), increasing from  $1182 \pm 50$   $\mu\text{m}$  in the control group to  $1250 \pm 79$   $\mu\text{m}$  in the pregnant group ( $P < 0.05$ ). This increase in diameter in the pregnant group may have occurred to accommodate the significant increase in cardiac output, as previously noted ([Fig. 2A](#)).

Additionally, inherent tissue stiffness decreased in both circumferential and axial directions of the pregnant DTA ([Fig. 4, C](#) and [F](#)) as compared to that of the control DTA (from  $1.90 \pm 0.16$  to  $1.68 \pm 0.25$  MPa in the circumferential direction and from  $2.34 \pm 0.30$  to  $1.84 \pm 0.50$  MPa in the axial direction,  $P < 0.05$  for both directions). Concurrently, wall thickness increased from  $36 \pm 2$  in the control to  $40 \pm 3$   $\mu\text{m}$  in the pregnant DTA ([Fig. 4H](#);  $P < 0.05$ ). Similarly, pregnancy was associated with increased structural distensibility ([Fig. 4I](#)) of the DTA (from  $19 \pm 2.4$  to  $21 \pm 2.2$   $\text{MPa}^{-1}$ ,  $P < 0.05$ ), despite no change observed in pulse pressure measurements (data not shown).

Furthermore, in-plane normal stresses along both directions of the pregnant DTA ([Fig. 4, B](#) and [E](#)) were lower when compared to the control group. In particular, the circumferential normal stress decreased from  $260 \pm 16$  kPa in the control group to  $234 \pm 22$  kPa in the pregnant group ( $P < 0.05$ ). In the axial direction, the normal stress dropped from  $255 \pm 21$  kPa in the control group to  $214 \pm 28$  kPa in the pregnant group ( $P < 0.05$ ).

## 4. Discussion

As maternal mortality rates continue to increase, and epidemiological evidence highlights the role of pregnancy history in predicting the future of the mother's cardiovascular health ([Hauspurg et al., 2018](#); [Wu et al., 2017](#)), it is crucial to understand the cardiovascular remodeling processes that occur throughout gestation. Herein, we report a functional assessment of the murine DTA from young C57BL/6 mice in the late-gestation period, to characterize changes in maternal hemodynamics and intrinsic wall mechanical properties independently.

In agreement with human hemodynamic studies during pregnancy ([Robson et al., 1989](#); [Poppas et al., 1997](#); [Clapp and Capeless, 1997](#)), cardiac output increased by approximately 50% in the pregnant group. Again aligned with clinical observations in human ([Robson et al., 1989](#); [Grindheim et al., 2012](#); [Katz et al., 1978](#)), our data showed no significant

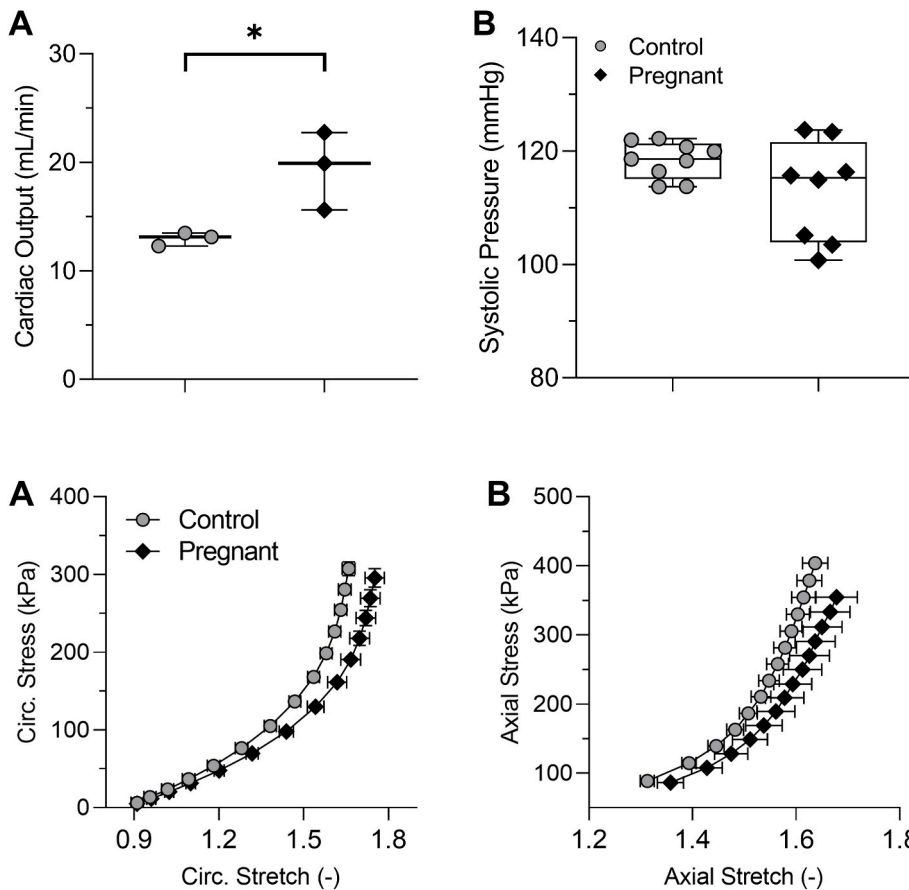


**Fig. 2.** Hemodynamics of age-matched control mice (gray circles) and late-gestation pregnant (black diamonds). (A) Cardiac Output (CO), calculated by cardiac echocardiograph readings of heart rate and stroke volume. (B) Systolic blood pressure. While there was an increase in CO, systolic blood pressure did not change between groups, similar to humans throughout gestation (Fig. 1A and B). As such, wild-type mice were deemed as an appropriate model for examining cardiovascular adaptations during pregnancy. Statistical significance was assessed by Mann-Whitney-Wilcoxon unpaired sample test for cardiac output measurements and Student's t-test for pressure measurements, with  $P \leq 0.05$  considered to be statistically significant.

**Fig. 3.** Experimental average mechanical response of tissues of the DTA, depicted by stress-stretch curves. Data are shown for age-matched control (gray circles,  $n = 9$ ) and late-gestation pregnant mice (black diamonds,  $n = 9$ ) in the mean (A) circumferential (Circ.) and (B) axial directions. The pregnant group experienced a rightward expansion of the stress stretch curve in both directions, indicative of global tissue softening. Error bars show SEM from experimental data collected on individual specimens.

change in blood pressure between both groups. As such, C57BL/6 mice were considered a physiologically and hemodynamically relevant model for examining cardiovascular remodeling during pregnancy.

An increase in the luminal diameter of the pregnant murine aorta measured at systolic blood pressure was observed, consistent with previous studies that reported an increase in aortic root diameter (East-erling et al., 1991) and a larger diameter during the late-gestation period (Hart et al., 1986) in humans. Langille et al. (Langille, 1993), explained how altered flow (specifically an increase in flow) appeared to modulate vascular changes during pregnancy, causing the aortic diameter to increase. As such, this increase in luminal diameter might be a remodeling response of the vessel to accommodate the increase in cardiac output, while maintaining constant blood pressure.

With preserved pressure and increased diameter, the vessel has to increase its wall thickness to avoid an increase in wall stress. Our results showed a 14% increase in wall thickness in the pregnant DTA. Wells et al. (Wells and Martin, 2022) previously explored alterations in the size of the DTA during pregnancy, though using a bovine model. Unlike our findings, their examinations revealed a relative reduction in tissue thickness during pregnancy in comparison to nulligravida control samples. It is plausible that this difference could have been due to measurements at earlier stages of pregnancy in their study. Wells and colleagues did not report during which level of gestation their measurements were taken. If such an examination was performed at earlier stages of pregnancy, the observed reduction in thickness of the aortic wall may plausibly denote a remodeling mechanism that takes place at an earlier stage of gestation, a phenomenon that we did not explore in our study. In addition, it is important to recognize that there is a likelihood of interspecies differences, given that our study employed a murine animal model as opposed to a bovine animal model.

Our findings showed that the pregnant tissue experienced softening

both in the axial and circumferential directions (Fig. 3). The softening of the pregnant tissue over a wide range of circumferential and axial deformations prevented a rise in intrinsic tissue stiffness under systolic loads during late-gestation (Fig. 4, C and F). Specifically, the intrinsic stiffness of the pregnant group appeared to be significantly lower than the nulligravida control tissue. Similarly, the structural stiffness—measured through the inverse metric of aortic distensibility—of the pregnant aorta was also lower than control (Fig. 4I). This observation is consistent with clinical studies which show a decrease in PWV during pregnancy, indicating a decrease in structural stiffness (Mersich et al., 2005; Turi et al., 2020).

The increase in wall thickness (Fig. 4H) during late-gestation pregnancy was in line with our initial hypothesis, which coupled with the increase in luminal diameter (Fig. 4G), would allow the aortic wall stress to be kept at its operating point. Surprisingly, our results showed that the aortic wall stress in the late-gestation group did not remain constant—rather it decreased significantly in the pregnant group (Fig. 4, B and E). Thus, the expansive remodeling of the aorta during pregnancy resulted in a reduction in biaxial wall stresses. Without further analysis of tissue micro-structure, we can only speculate how the remodeling process led to a decrease in the wall stress of pregnant tissue. It is possible that the remodeling of the aortic wall during late gestation was an “overshoot” response during that relatively short timeframe. The reduction of stress could also be aimed at preventing excessive stresses during labor and delivery. We did not conduct any tests to assess blood pressure or vascular tissue properties during labor, delivery, or the postpartum period. However, previous research has indicated that blood pressure tends to increase during labor (Cohen et al., 2015), which, when coupled with the observed remodeling, could result in an increase in aortic wall stress. Therefore, it is conceivable that the decrease in stress and softening of the tissue during late gestation served as a

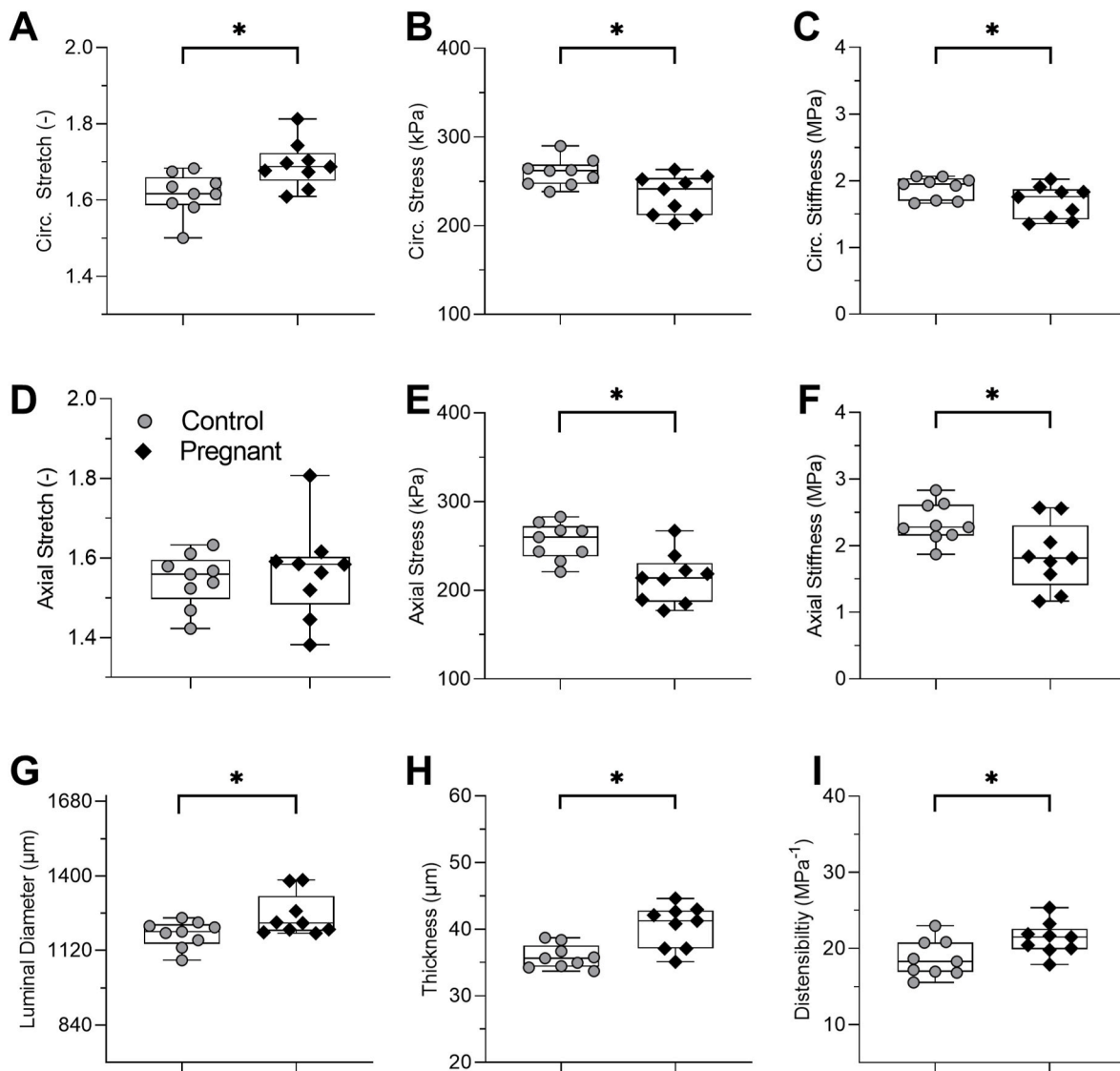


**Fig. 4.** Structural and material parameters of the DTA of age-matched nulligravida control mice (gray circles,  $n = 9$ ) and late-gestation pregnant mice (black diamonds,  $n = 9$ ). (A) Circumferential (Circ.) stretch. (B) Circumferential stress. (C) Circumferential stiffness. (D) Axial stretch. (E) Axial stress. (F) Axial stiffness. (G) Luminal diameter. (H) Wall thickness. (I) Distensibility. Calculations of stretch, stress, stiffness, luminal diameter and wall thickness were performed at group-specific systolic blood pressure measurements. Distensibility measures for structural stiffness and accounts for diameter and pressure changes between diastole and systole. The thickening of the wall in the late-gestation group, coupled with the increase in luminal diameter and the tissue softening, decreased the intrinsic stiffness in both the axial and circumferential directions. Similarly, the significant thickening of the wall in the pregnant group reduced the wall stress to lower values when compared to the control group, by outpacing the increase in luminal diameter. The asterisk (\*) represents a statistically significant difference of  $P < 0.05$ .

mechanism to prevent vascular damage during labor, delivery, and/or the postpartum period.

In summary, the objective of this study was to elucidate the biomechanical response of the murine DTA during a normotensive pregnancy in the late-gestational phase. Despite the lack of noteworthy changes in blood pressure, the aorta displayed an increase in size, as evidenced by the augmented luminal diameter and increased wall thickness. This widening and thickening of the aorta resulted in a reduction of tensile wall stress. Moreover, the geometric remodeling led to a reduction in the structural stiffness of the aorta, with augmented ability to expand in response to in-vivo loads. Therefore, our study reports for the first time a comprehensive view of the biomechanical mechanisms (i.e., reduction in intrinsic stiffness) associated with pregnancy-induced changes in the structure and function of the aorta in mice. Additionally, it establishes crucial baseline data to further evaluate the cardiovascular consequences of different medical conditions during the late stages of pregnancy, such as preeclampsia, and their potential impact on the aorta.

Given the projected increases in maternal mortality rate over the next few years and our knowledge gap both in normotensive pregnancies as well as in pathophysiological conditions during pregnancy, more biomechanical and mechanobiological research in the field of cardio-obstetrics is necessary.

#### CRediT authorship contribution statement

**Ana I. Vargas:** Conceptualization, Formal analysis, Investigation, Data curation, Writing – original draft, Writing – review & editing, Visualization. **Samar A. Tarraf:** Formal analysis, Software, Writing – review & editing. **Timothy P. Fitzgibbons:** Investigation, Writing – review & editing. **Chiara Bellini:** Conceptualization, Methodology, Resources, Writing – review & editing, Supervision. **Rouzbah Amini:** Conceptualization, Resources, Writing – review & editing, Supervision, Project administration, Funding acquisition.

## Declaration of competing interest

The authors declare no conflicts of interest related to the research and publication of this paper.

## Data availability

Data will be made available on request.

## Appendix A

Consistent with our previously published work (Nwotchouang et al., 2021; Thomas et al., 2019; Clarin et al., 2023) and as part of our efforts to broaden the impact of our research, we have developed an educational component related to the research work discussed in this manuscript. The “homework problem” presented herein aims to provide a deeper insight into the biomechanics of the aortic wall and is appropriate for an undergraduate level biomechanics course.

**Problem** - Luminal pressure in blood vessels generates tensile stresses within the plane of the vessel wall (Fig. A.5). In our paper, the circumferential wall stress ( $\sigma_{circ}$ ) was calculated via the law of Laplace

$$\sigma_{circ} = \frac{Pr}{h} \quad (A.1)$$

where  $r$  and  $h$  are the luminal radius and the wall thickness in the loaded configuration, respectively. The law of Laplace, postulates that the tension in the wall is directly proportional to the product of pressure and luminal radius assuming, for simplification purposes, that the aorta is a thinned-walled cylinder (Fig. A.5) (Westerhof et al., 2010).

In the first part of the problem, determine the percentage change in circumferential wall stress at systolic blood pressure between the late-gestation group and the age-matched control group. The average values needed for this calculation can be found in Table A.1.

The second objective is to comprehend the impact of hypertensive pregnancies on tensile wall stress. Hypertension is a frequently observed complication during pregnancy and can lead to serious health issues for both mother and fetus. Approximately 10% of all pregnancies are affected by hypertension (Garovic, 2000). Therefore, to understand how hypertension affects the biomechanics of the aorta, calculate the circumferential wall stress ratio

$$\frac{\sigma_{circ,hypertensive}}{\sigma_{circ,nulligravida}} \quad (A.2)$$

and compare it to the wall stress ratio of normotensive and nulligravida mice. Assume that all parameters stay the same between normotensive and hypertensive mice, and the systolic blood pressure in the hypertensive model is: 140 mmHg. Discuss the effects of an elevated high blood pressure in pregnancy, and explore the potential impacts that the changes in the geometry of the vessel might have on the aortic wall stress.

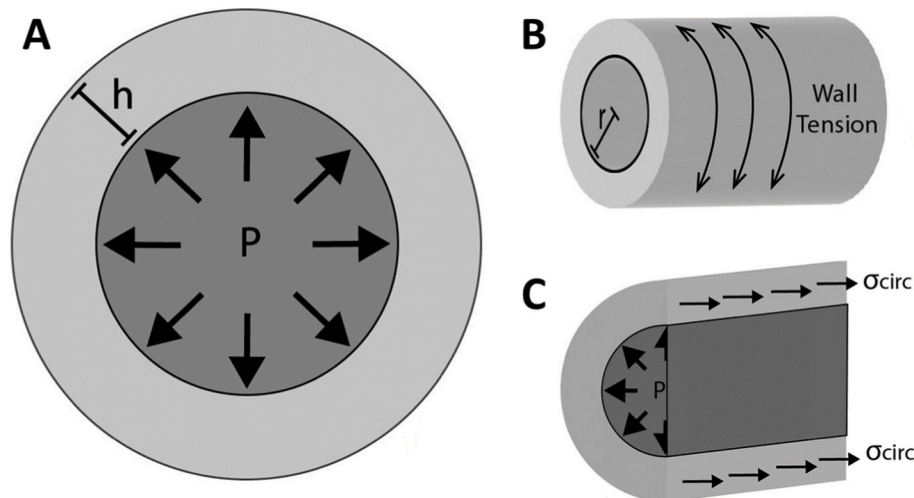


**Fig. A.5.** Law of Laplace Diagram. This law describes the relationship between pressure and wall stress in thin structures when the radius of curvature of the curved surface and its thickness are known. (A) Cross-sectional top view of a cylinder illustrating the pressure ( $P$ ) acting on the inner wall, and the thickness ( $h$ ) of the wall. (B) Side view of a cylinder, illustrating the tension produced on the wall when pressure is applied.  $r$  denotes the luminal radius of the cylinder. (C) Cross-section side view of a cylinder, illustrating the circumferential wall stress ( $\sigma_{circ}$ ) acting on the wall as pressure is applied.

**Table A.1**

Average raw data collected for the late-gestation pregnant group and age-matched controls at their respective systolic blood pressure.

Groups	Systolic Pressure (mmHg)	h ( $\mu\text{m}$ )	Luminal Diameter ( $\mu\text{m}$ )
Control	118	36	1182
Late Gestation	113	40	1250

## References

- Baek, S., Gleason, R.L., Rajagopal, K., Humphrey, J., 2007. Theory of small on large: potential utility in computations of fluid–solid interactions in arteries. *Comput. Methods Appl. Mech. Eng.* 196 (31–32), 3070–3078. <https://doi.org/10.1016/j.cma.2006.06.018>.
- Blum, J.L., Chen, L.-C., Zelikoff, J.T., 2017. Exposure to ambient particulate matter during specific gestational periods produces adverse obstetric consequences in mice. *Environ. Health Perspect.* 125 (7), 077020 <https://doi.org/10.1289/EHP1029>.
- Buchan, P.C., 1984. Maternal and fetal blood viscosity throughout normal pregnancy. *J. Obstet. Gynaecol.* 4 (3), 143–150. <https://doi.org/10.3109/01443618409075702>.
- Cardillo, G., 2009. *Mwtest: Mann-Whitney-Wilcoxon Non Parametric Test for Two Unpaired Samples*.
- Clapp, J.F., Capeless, E., 1997. Cardiovascular function before, during, and after the first and subsequent pregnancies. *Am. J. Cardiol.* 80 (11), 1469–1473. [https://doi.org/10.1016/S0002-9149\(97\)00738-8](https://doi.org/10.1016/S0002-9149(97)00738-8).
- Clarín, J., Dang, D., Santos, L., Amini, R., 2023. Mechanical characterization of porcine tricuspid valve anterior leaflets over time: applications to ex vivo studies. *ASME Open Journal of Engineering* 2 (1). <https://doi.org/10.1115/1.4062477>.
- Coccolone, A.J., Hawes, J.Z., Staiculescu, M.C., Johnson, E.O., Murshed, M., Wagenseil, J.E., 2018. Elastin, arterial mechanics, and cardiovascular disease. *Am. J. Physiol. Heart Circ. Physiol.* 315, H189–H205. <https://doi.org/10.1152/AJPHEART.00087.2018>. URL: [www.ajpheart.org](http://www.ajpheart.org).
- Cohen, J., Vaiman, D., Sibai, B.M., Haddad, B., 2015. Blood pressure changes during the first stage of labor and for the prediction of early postpartum preeclampsia: a prospective study. *Eur. J. Obstet. Gynecol. Reprod. Biol.* 184, 103–107.
- Davidson, D., 1989. *The house mouse: atlas of embryonic development*. by k. theiler. second printing, 1989. new york: Springer-verlag. 178 pages. dm 168.00. isbn 3 540059407 *Genetics Research* 54 (3), 240–241. <https://doi.org/10.1017/S001667230002872X>.
- Duley, L., 2009. The global impact of pre-eclampsia and eclampsia. *Semin. Perinatol.* 33, 130–137. <https://doi.org/10.1053/J.SEMPERI.2009.02.010>.
- Easterling, T.R., Benedetti, T.J., Schmucker, B.C., Carlson, K., Millard, S.P., 1991. Maternal hemodynamics and aortic diameter in normal and hypertensive pregnancies. *Obstet. Gynecol.* 78 (6), 1073–1077.
- Estensen, M.-E., Remme, E.W., Grindheim, G., Smiseth, O.A., Segers, P., Henriksen, T., Aakhus, S., 2013. Increased arterial stiffness in pre-eclamptic pregnancy at term and early and late postpartum: a combined echocardiographic and tonometric study. *Am. J. Hypertens.* 26 (4), 549–556. <https://doi.org/10.1093/AJH/HPS067>.
- Farra, Y.M., Matz, J., Ramkhalawon, B., Oakes, J.M., Bellini, C., 2021. Structural and functional remodeling of the female ApoE<sup>-/-</sup> mouse aorta due to chronic cigarette smoke exposure. *Am. J. Physiol. Heart Circ. Physiol.* 320 (6), H2270. <https://doi.org/10.1152/AJPHEART.00893.2020>. –H2282.
- Ferruzzi, J., Bersi, M.R., Humphrey, J.D., 2013. Biomechanical phenotyping of central arteries in health and disease: advantages of and methods for murine models. *Ann. Biomed. Eng.* 41, 1311–1330. <https://doi.org/10.1007/s10439-013-0799-1>.
- Franz, M.B., Burgmann, M., Neubauer, A., Zeisler, H., Sanani, R., Gottsauner-Wolf, M., Schiessl, B., Andreas, M., 2013. Augmentation index and pulse wave velocity in normotensive and pre-eclamptic pregnancies. *Acta Obstet. Gynecol. Scand.* 92 (8), 960–966. <https://doi.org/10.1111/AOGS.12145>.
- Garovic, V.D., 2000. Hypertension in pregnancy: diagnosis and treatment. In: *Mayo Clinic Proceedings*, vol. 75. Elsevier, pp. 1071–1076.
- Gleason, R., Gray, S., Wilson, E., Humphrey, J., 2004. A multiaxial computer-controlled organ culture and biomechanical device for mouse carotid arteries. *J. Biomech. Eng.* 126 (6), 787–795. <https://doi.org/10.1115/1.1824130>.
- Grindheim, G., Estensen, M.E., Langesaeter, E., Rosseland, L.A., Toska, K., 2012. Changes in blood pressure during healthy pregnancy: a longitudinal cohort study. *J. Hypertens.* 30 (2), 342–350. <https://doi.org/10.1097/HJH.0B013E32834F0B1C>.
- Groenink, M., de Roos, A., Mulder, B.J., Spaan, J.A., van der Wall, E.E., 1998. Changes in aortic distensibility and pulse wave velocity assessed with magnetic resonance imaging following beta-blocker therapy in the marfan syndrome. *Am. J. Cardiol.* 82 (2), 203–208. [https://doi.org/10.1016/S0002-9149\(98\)00315-4](https://doi.org/10.1016/S0002-9149(98)00315-4).
- Hart, M.V., Morton, M.J., Hosenpud, J.D., Metcalfe, J., 1986. Aortic function during normal human pregnancy. *Am. J. Obstet. Gynecol.* 154 (4), 887–891.
- Hauspurg, A., Ying, W., Hubel, C.A., Michos, E.D., Ouyang, P., 2018. Adverse pregnancy outcomes and future maternal cardiovascular disease. *Clin. Cardiol.* 41 (2), 239–246. <https://doi.org/10.1002/clc.22887>.
- Huisman, A., Aarnoudse, J.G., Huisjes, H.J., Fidler, V., Zijlstra, W.G., Heuvelmans, J.H., Goslinga, H., 1987. Whole blood viscosity during normal pregnancy. *BJOG An Int. J. Obstet. Gynaecol.* 94 (12), 1143–1149. <https://doi.org/10.1111/J.1471-0528.1987.TB02313.X>.
- Hunter, S., Robson, S.C., 1992. Adaptation of the maternal heart in pregnancy. *Br. Heart J.* 68, 540. <https://doi.org/10.1136/HRT.68.12.540>.
- Jondeau, G., Boutouyrie, P., Lacombe, P., Laloux, B., Dubourg, O., Bourdarias, J.-P., Laurent, S., 1999. Central pulse pressure is a major determinant of ascending aorta dilation in marfan syndrome. *Circulation* 99 (20), 2677–2681. <https://doi.org/10.1161/01.CIR.99.20.2677>.
- Kager, C.C., Dekker, G.A., Stam, M.C., 2009. Measurement of cardiac output in normal pregnancy by a non-invasive two-dimensional independent Doppler device, Australian and New Zealand. *J. Obstet. Gynaecol.* 49 (2), 142–144. <https://doi.org/10.1111/J.1479-828X.2009.00948.X>.
- Katz, R., Karliner, J.S., Resnik, R., 1978. Effects of a natural volume overload state (pregnancy) on left ventricular performance in normal human subjects. *Circulation* 58 (3 Pt 1), 434–441. <https://doi.org/10.1161/01.cir.58.3.434>.
- Langille, L.B., 1993. Remodeling of developing and mature arteries: endothelium, smooth muscle, and matrix. *J. Cardiovasc. Pharmacol.* 21, S11–S17.
- Mersich, B., Rigó Jr., J., Besenyei, C., Lénárd, Z., Studinger, P., Kollai, M., 2005. Opposite changes in carotid versus aortic stiffness during healthy human pregnancy. *Clin. Sci.* 109 (1), 103–107. <https://doi.org/10.1042/CS20040352>.
- Mulder, E.G., de Haas, S., Mohseni, Z., Schartmann, N., Abo Hasson, F., Alsadah, F., van Kuijk, S.M., van Dronghen, J., Spaanderman, M.E., Ghossein-Doha, C., 2022. Cardiac output and peripheral vascular resistance during normotensive and hypertensive pregnancy – a systematic review and meta-analysis. *BJOG An Int. J. Obstet. Gynaecol.* 129 (5), 696–707. <https://doi.org/10.1111/1471-0528.16678>.
- Nwotchouang, B.S.T., Eppelheimer, M.S., Biswas, D., Pahlavian, S.H., Zhong, X., Oshinski, J.N., Barrow, D.L., Amini, R., Loth, F., 2021. Accuracy of cardiac-induced brain motion measurement using displacement-encoding with stimulated echoes (dense) magnetic resonance imaging (mri): a phantom study. *Magn. Reson. Med.* 85 (3), 1237–1247.
- Oosterhof, H., Wichers, G., Fidler, V., Aarnoudse, J.G., 1993. Blood viscosity and uterine artery flow velocity waveforms in pregnancy: a longitudinal study. *Placenta* 14 (5), 555–561. [https://doi.org/10.1016/S0143-4004\(05\)80208-5](https://doi.org/10.1016/S0143-4004(05)80208-5).
- Osman, M.W., Nath, M., Khalil, A., Webb, D.R., Robinson, T.G., Mousa, H.A., 2017. Longitudinal study to assess changes in arterial stiffness and cardiac output parameters among low-risk pregnant women. *Pregnancy Hypertension* 10, 256–261. <https://doi.org/10.1016/j.pregHY.2017.10.007>.
- Petersen, E.E., Davis, N.L., Goodman, D., Cox, S., Mayes, N., Johnston, E., Syverson, C., Seed, K., Shapiro-Mendoza, C.K., Callaghan, W.M., Barfield, W., 2019. Vital signs: pregnancy-related deaths, United States, 2011–2015, and strategies for prevention, 13 states, 2013–2017. *MMWR (Morb. Mortal. Wkly. Rep.)* 68, 423. <https://doi.org/10.15585/MMWR.MM6818E1>.
- Pierlot, C.M., Lee, J.M., Amini, R., Sacks, M.S., Wells, S.M., 2014. Pregnancy-induced remodeling of collagen architecture and content in the mitral valve. *Ann. Biomed. Eng.* 42 (10), 2058–2071. <https://doi.org/10.1007/s10439-014-1077-6>.
- Pierlot, C.M., Moeller, A.D., Lee, J.M., Wells, S.M., 2015. Pregnancy-induced remodeling of heart valves. *Am. J. Physiol. Heart Circ. Physiol.* 309 (9), H1565–H1578. <https://doi.org/10.1152/ajpheart.00816.2014>. Recent.
- Poppas, A., Shroff, S.G., Korcarz, C.E., Hibbard, J.U., Berger, D.S., Lindheimer, M.D., Lang, R.M., 1997. Serial assessment of the cardiovascular system in normal pregnancy. *Circulation* 95 (10), 2407–2415. <https://doi.org/10.1161/01.CIR.95.10.2407>.
- Ramlakhan, K.P., Johnson, M.R., Roos-Hesselink, J.W., 2020. Pregnancy and cardiovascular disease. *Nat. Rev. Cardiol.* 17, 718–731. <https://doi.org/10.1038/S41569-020-0390-Z>.
- Regitz-Zagrosek, V., Roos-Hesselink, J.W., Bauersachs, J., Blomström-Lundqvist, C., Cifkova, R., De Bonis, M., Lung, B., Johnson, M.R., Kintscher, U., Kranke, P., et al., 2018. Esc guidelines for the management of cardiovascular diseases during pregnancy: the task force for the management of cardiovascular diseases during pregnancy of the european society of cardiology (esc). *Eur. Heart J.* 39 (34), 3165–3241. <https://doi.org/10.1093/EURHEARTJ/EHY340>, 2018.
- Respress, J.L., Wehrens, X.H., 2010. Transthoracic echocardiography in mice. *J. Vis. Exp.* 1738doi <https://doi.org/10.3791/1738>.
- Robson, S.C., Hunter, S., Boys, R.J., Dunlop, W., 1989. Serial study of factors influencing changes in cardiac output during human pregnancy. *Am. J. Physiol.* 256 (4 Pt 2) <https://doi.org/10.1152/AJPHEART.1989.256.4.H1060>.
- Rodriguez, C., Chi, Y.Y., Chiu, K.H., Zhai, X., Lingis, M., Williams, R.S., Rhoton-Vlasak, A., Nichols, W.W., Petersen, J.W., Segal, M.S., Conrad, K.P., Mohandas, R., 2018. Wave reflections and global arterial compliance during normal human pregnancy. *Physiological Reports* 6 (24), e13947. <https://doi.org/10.14814/PHY2.13947>.
- Scherrer-Crosbie, M., Thibault, H.B., 2008. Echocardiography in translational research: of mice and men. *J. Am. Soc. Echocardiogr.* 21 (10), 1083–1092. <https://doi.org/10.1016/j.echo.2008.07.001>.
- Thomas, V.S., Lai, V., Amini, R., 2019. A computational multi-scale approach to investigate mechanically-induced changes in tricuspid valve anterior leaflet microstructure. *Acta Biomater.* 94, 524–535.

- Thornburg, K.L., Jacobson, S.L., Giraud, G.D., Morton, M.J., 2000. Hemodynamic changes in pregnancy. *Semin. Perinatol.* 24, 11–14. [https://doi.org/10.1016/S0146-0005\(00\)80047-6](https://doi.org/10.1016/S0146-0005(00)80047-6).
- Torrado, J., Farro, I., Zócalo, Y., Farro, F., Sosa, C., Scasso, S., Alonso, J., Bia, D., 2015. Preeclampsia is associated with increased central aortic pressure, elastic arteries stiffness and wave reflections, and resting and recruitable endothelial dysfunction. *Int. J. Hypertens.* 2015. <https://doi.org/10.1155/2015/720683>.
- Turi, V., Dragan, S., Iurciuc, M., Moleriu, L., Bungau, S., Tit, D.M., Toader, D.-O., Diaconu, C.C., Behl, T., Petre, I., 2020. Arterial function in healthy pregnant women vs. non-pregnant women—a 10-year study. *Diagnostics* 10 (6), 374. <https://doi.org/10.3390/DIAGNOSTICS10060374>.
- Wagenseil, J.E., Mecham, R.P., 2009. Vascular extracellular matrix and arterial mechanics. *Physiol. Rev.* 89, 957–989. <https://doi.org/10.1152/PHYSREV.00041.2008>. URL. [www.prv.org](http://www.prv.org).
- Weizsäcker, H.W., Lambert, H., Pascale, K., 1983. Analysis of the passive mechanical properties of rat carotid arteries. *J. Biomech.* 16, 703–715. [https://doi.org/10.1016/0021-9290\(83\)90080-5](https://doi.org/10.1016/0021-9290(83)90080-5).
- Wells, S., Martin, M., 2022. Remodeling of bovine descending aorta and aortic valve during pregnancy are not reversed postpartum. *Can. J. Cardiol.* 38 (10), S112. <https://doi.org/10.1016/j.cjca.2022.08.035>.
- Westerhof, N., Stergiopulos, N., Stergiopulos, N., Noble, M., 2010. Law of Laplace, pp. 45–48. [https://doi.org/10.1007/978-1-4419-6363-5\\_9](https://doi.org/10.1007/978-1-4419-6363-5_9).
- Wu, P., Haththotuwa, R., Kwok, C.S., Babu, A., Kotronias, R.A., Rushton, C., Zaman, A., Fryer, A.A., Kadam, U., Chew-Graham, C.A., et al., 2017. Preeclampsia and future cardiovascular health: a systematic review and meta-analysis. *Circulation: Cardiovascular Quality and Outcomes* 10 (2), e003497.
- Zentner, D., Wheeler, M., Grigg, L., 2012. Does pregnancy contribute to systemic right ventricular dysfunction in adults with an atrial switch operation? *Heart Lung Circ.* 21 (8), 433–438. <https://doi.org/10.1016/J.HLC.2012.04.009>.